Supporting Information

Porous organic cage crystals: characterising the porous crystal surface

Michael J. Bojdys,[a] Tom Hasell,[a] Nikolai Severin,[b] Kim E. Jelfs,[a] Jürgen P. Rabe[b] and Andrew I. Cooper*[a]

[a]Department of Chemistry and Centre for Materials Discovery, University of Liverpool, Crown Street, Liverpool L69 7ZD, United Kingdom.

[b]Humboldt-Universität zu Berlin, Institut für Physik, Newtonstraße 15, 12489 Berlin, Germany.

Supporting Information Available. Synthetic procedures, characterisation and modeling details, SEM and AFM images and analysis.

Characterization.

Scanning Electron Microscopy. High resolution imaging of the crystal morphology was achieved using a Hitachi S-4800 cold Field Emission Scanning Electron Microscope (FE-SEM). The dry samples were prepared on 15 mm Hitachi M4 aluminium stubs using an adhesive high purity carbon tab. The samples were then coated with a 2 nm layer of gold using an Emitech K550X automated sputter coater.

Scanning force microscopy. Scanning force microscopy (SFM) was performed under ambient conditions with a Nanoscope 3a (Veeco) instrument in tapping mode with silicon cantilevers (Olympus, Japan) with a typical resonant frequency of 70 kHz and a spring constant of about 2 N/m and in contact mode with the tips used for tapping mode and silicon nitride cantilevers (Veeco) with a typical spring constant of 12 N/m.

Surface relaxation modelling: Models of the surface topology were constructed by cleaving the crystal to the respective Miller index, with two layers to represent the surface and 3 layers which were fixed to represent the bulk crystal. The surfaces were modelled as an aperiodic 2D cell. The surfaces were then geometry optimised using our in-house forcefield, specifically parameterised for porous organic imine cages (including **CC3**),[1] with a second-order minimisation algorithm and a convergence criteria of 0.00001 kcal/(mol Ang), to allow surface relaxation. No observable surface relaxation occurred for either surface.

Synthesis of CC3-*R*: Crystals of **CC3**-*R* were obtained with the same procedure as described in literature.[2]

Preparation of CC3-*R* for AFM measurements: Crystals of **CC3**-*R* were fragmented with a clean razor blade, and a subset of crystallites exposing smooth planes in optical microscopy was selected. Crystallites were affixed via double sided adhesive tape (Tesa, Doppelband Fotostrip) onto a sample holder (AFM Specimen Disc, 12 mm diameter, Ted Pella, Inc.), and the AFM tip was positioned over the flat surfaces. AFM measurements were performed on flat surfaces up to one hour after producing the fragments and took a total of ~6 hours.

Fig. S 1 Scanning electron microscope images of crystals of **CC3**-*R*.

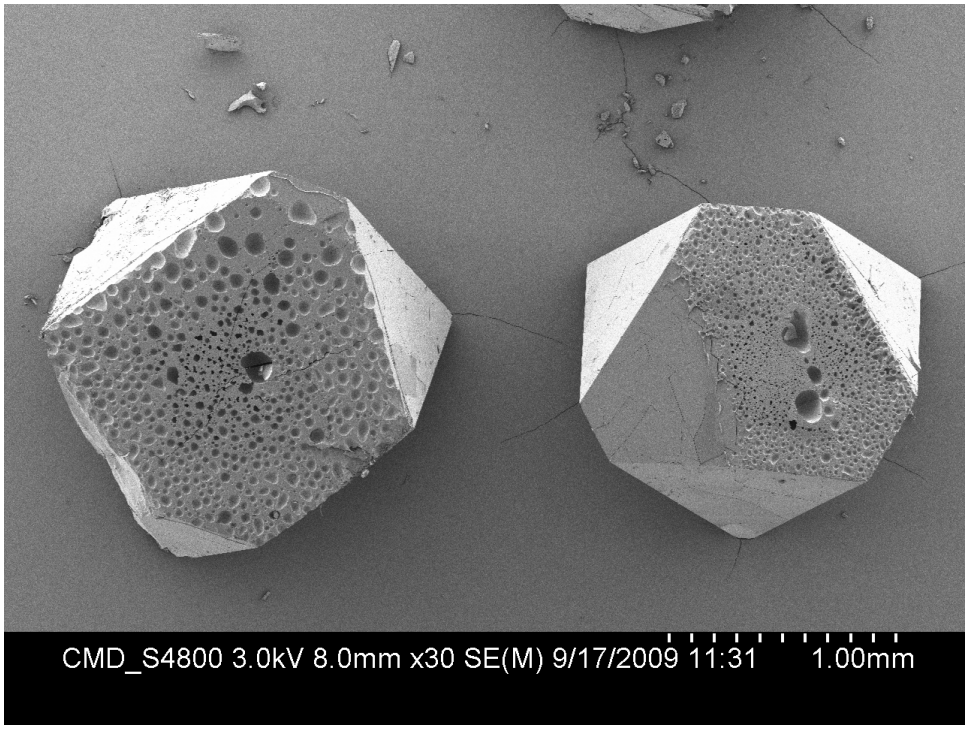

Fig. S 2 Scanning electron microscope images of crystals of **CC3**-*R*.

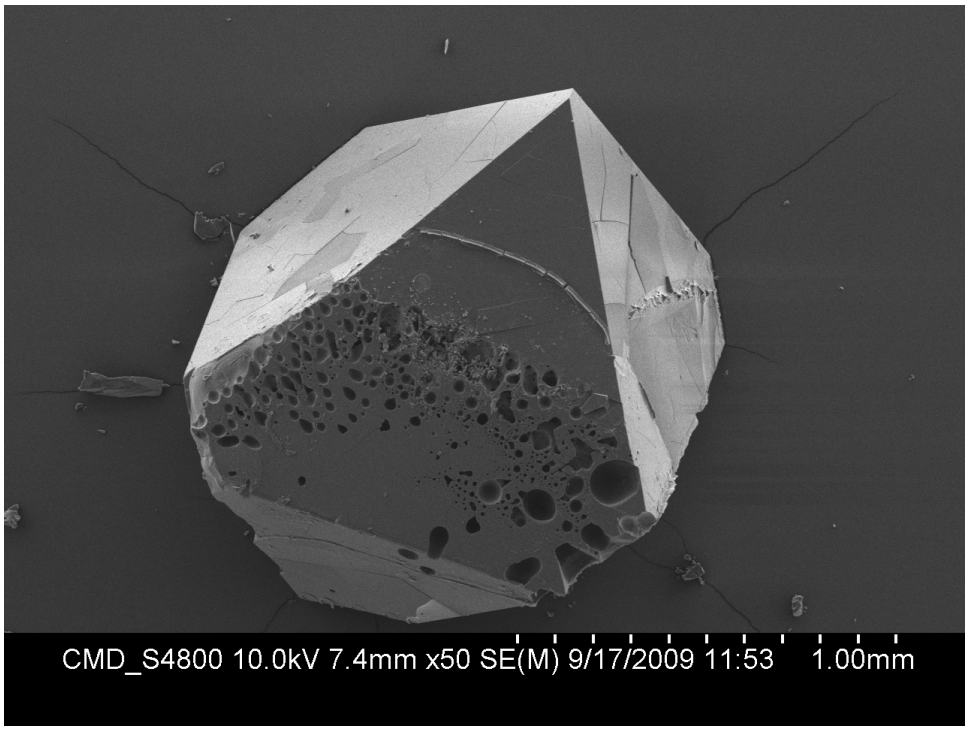

Fig. S 3 Scanning electron microscope images of crystals of **CC3**-*R*.

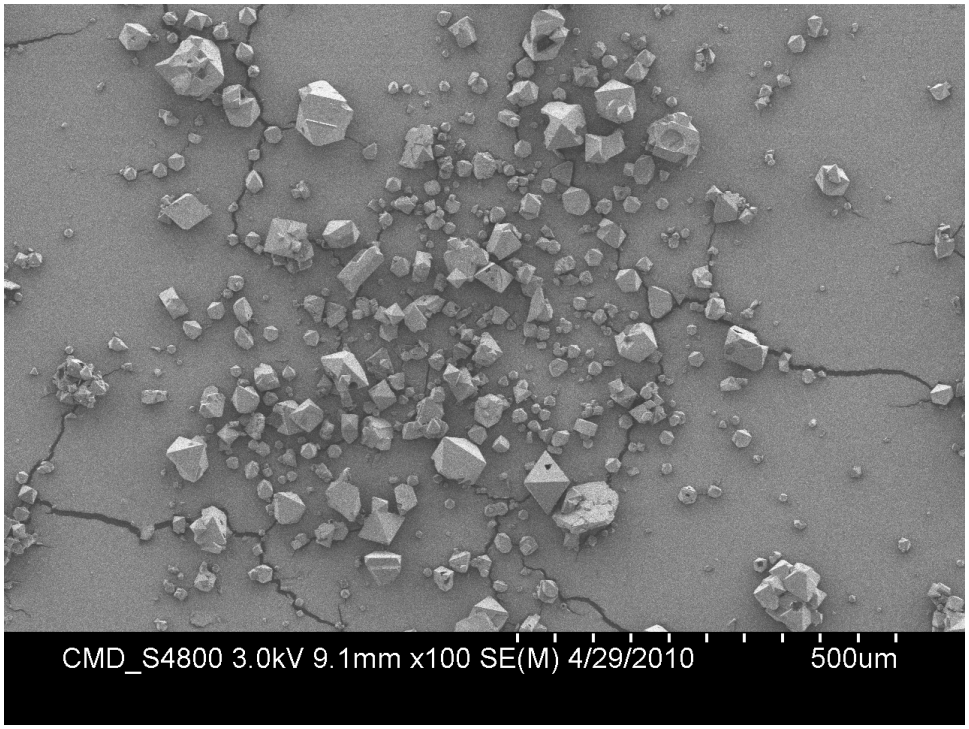

Fig. S 4 Scanning electron microscope images of crystals of **CC3**-*R*.

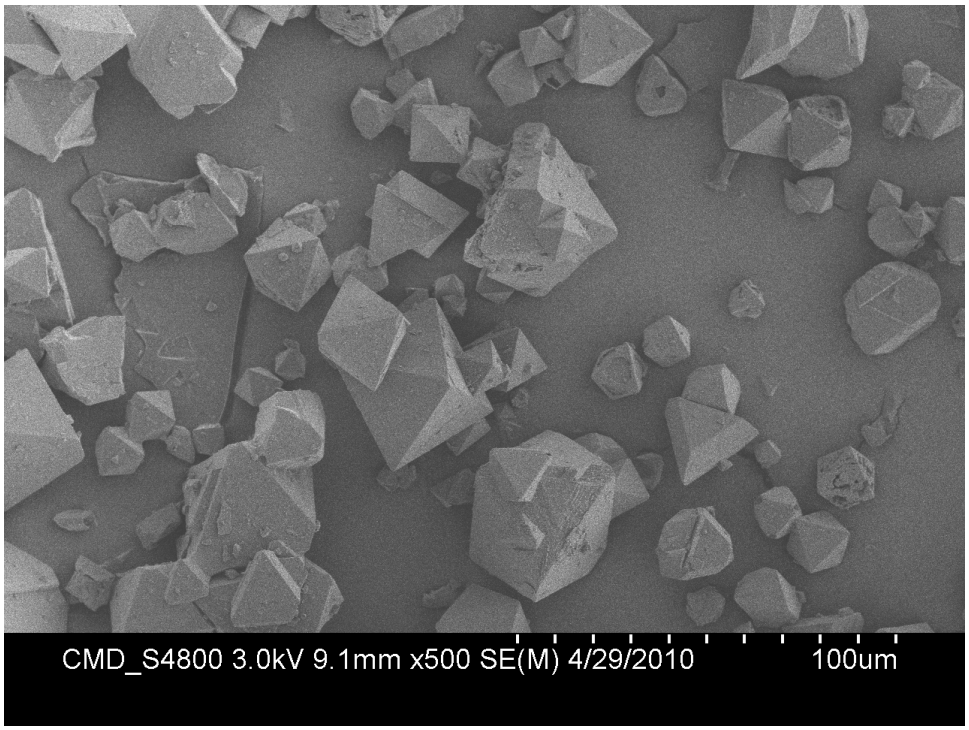

Fig. S 5 Atomic force microscopy (AFM) images of **CC3**-*R*, (a) showing large scan area topography and (b) simultaneously amplitude images.

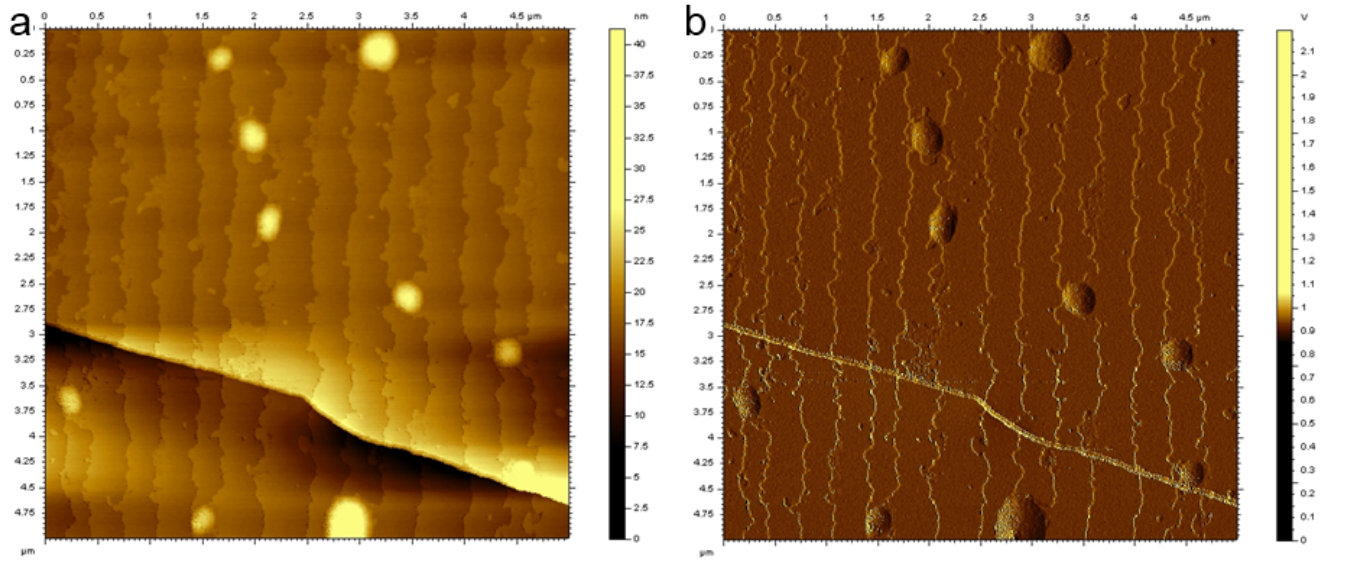

Fig. S 6 Atomic force microscopy (AFM) images of **CC3**-*R*, (a) showing large scan area recorded in tapping mode. (b) No damage of the surface by previous long time scanning in the center as seen in contact mode.

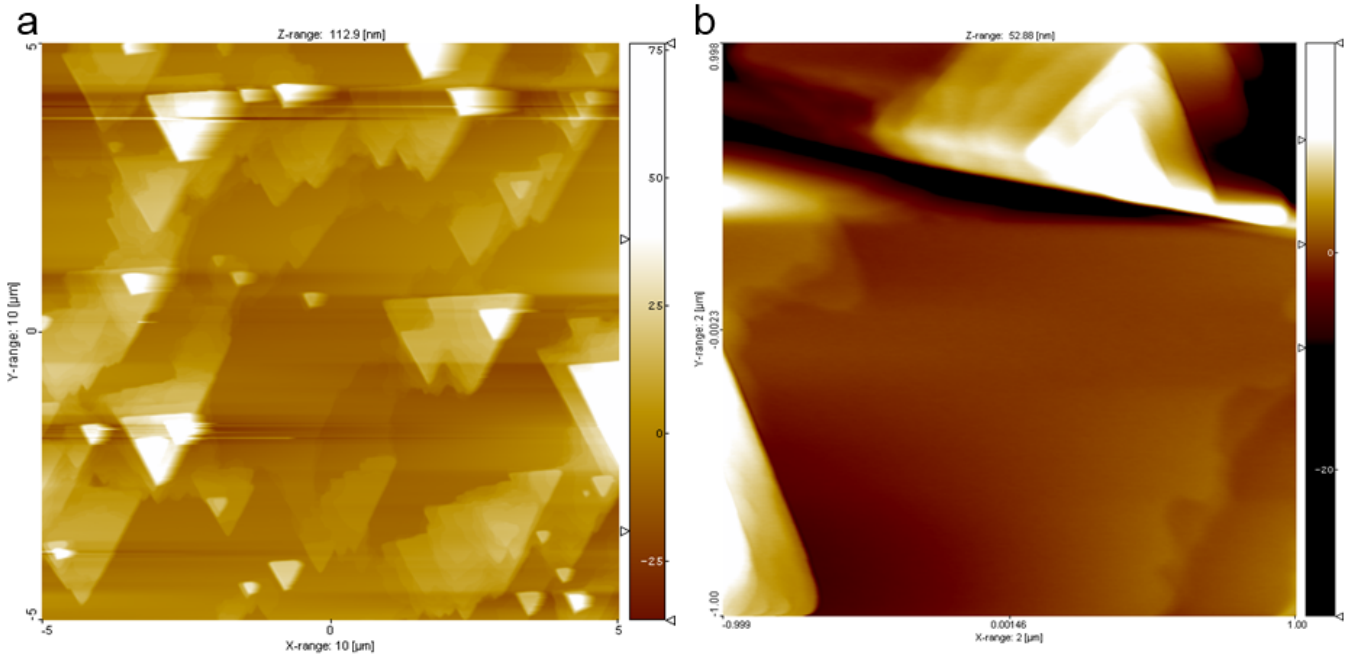

Fig. S 7 Atomic force microscopy (AFM) images of **CC3**-*R*, (a) showing topography and (b) simultaneously recorded friction images. Insets show Fourier-transforms of the whole collected region. In each case a hexagonal unit cell with ~1.7 m sides is verified.

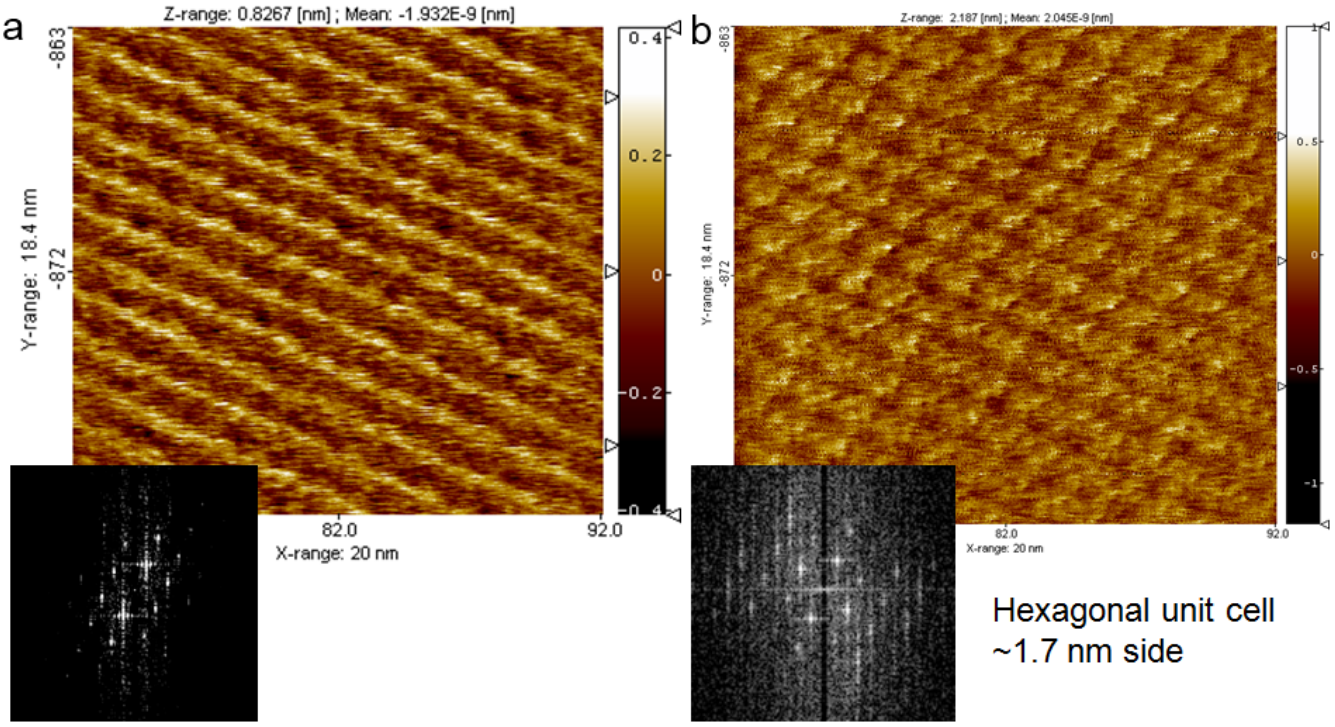

Fig. S 8 Atomic force microscopy (AFM) images of **CC3**-*R*, (a) showing contact mode topography with hexagonal unit cell (~1.7 nm sides) and (b) switching directions and scan size during image acquisition, verifying that observed structures are real.

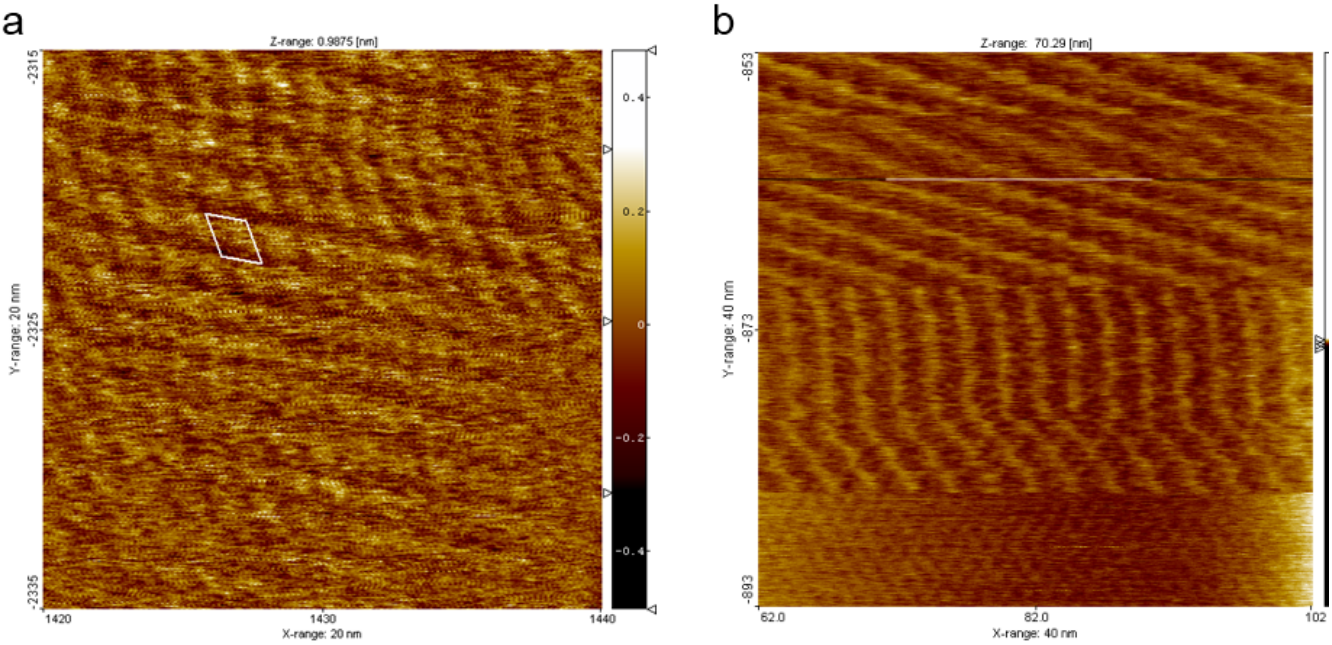

Fig. S 9 Representative AFM images of **CC3**-*R*, (a) showing contact mode topography and (b) simultaneously recorded friction images.

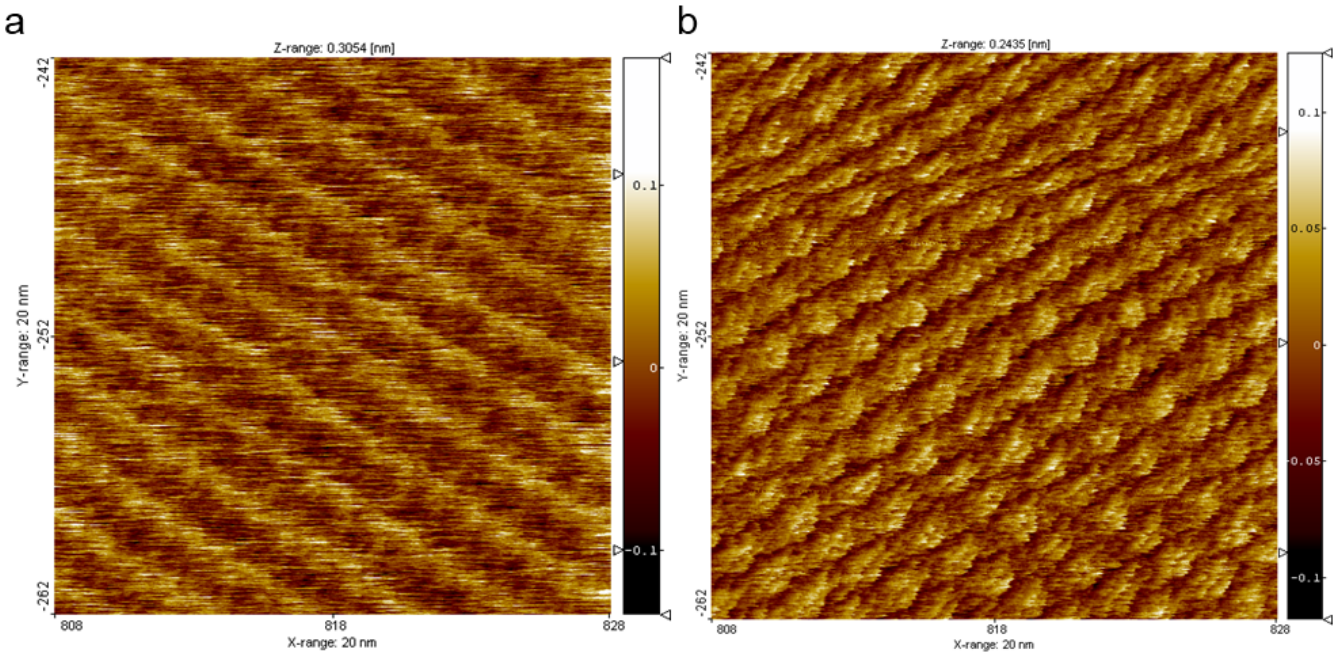

Fig. S 10 Representative AFM images of **CC3**-*R*, (a) showing contact mode topography and (b) simultaneously recorded friction images.

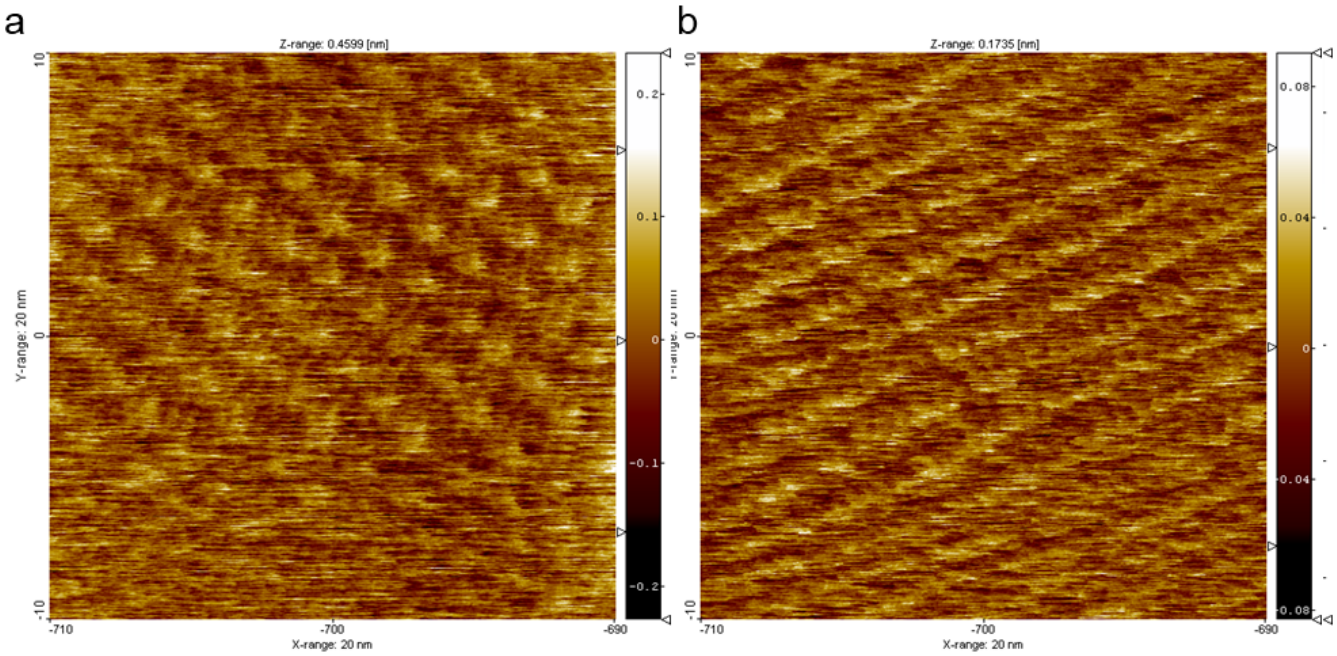

Fig. S 11 Representative AFM images of **CC3**-*R*, (a) showing contact mode topography and (b) simultaneously recorded friction images.

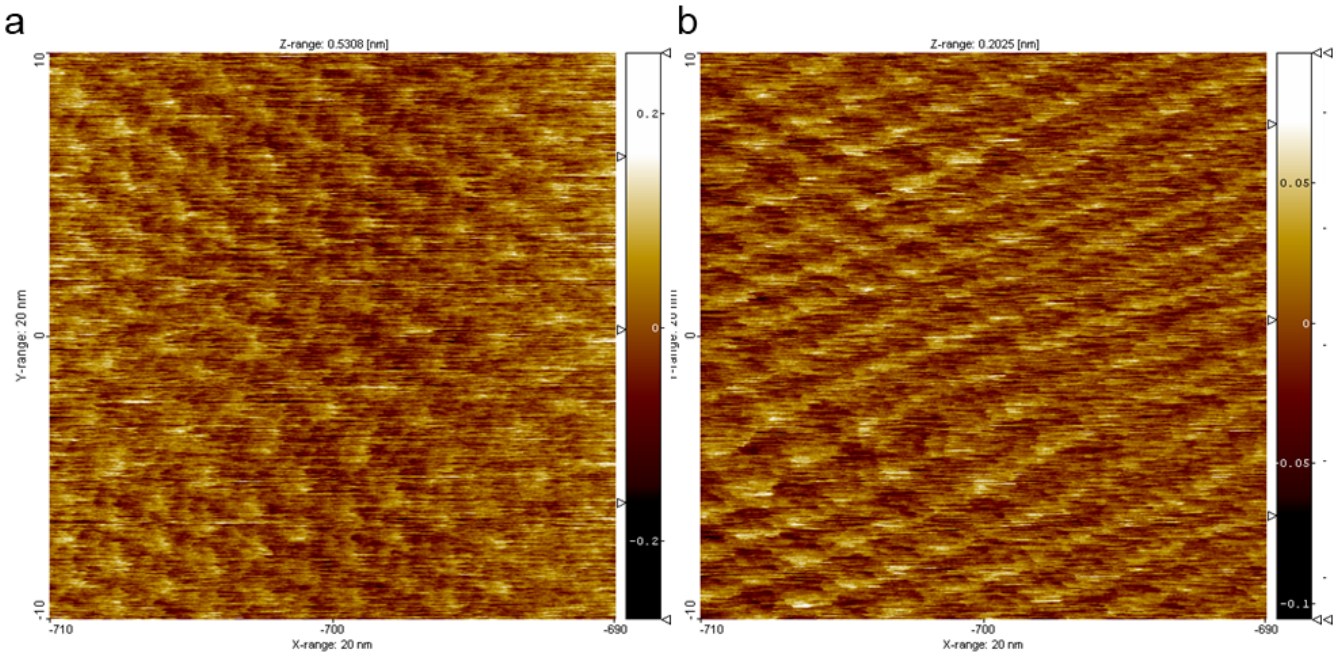

Fig. S 12 Representative AFM images of **CC3**-*R*, (a) showing contact mode topography and (b) simultaneously recorded friction images.

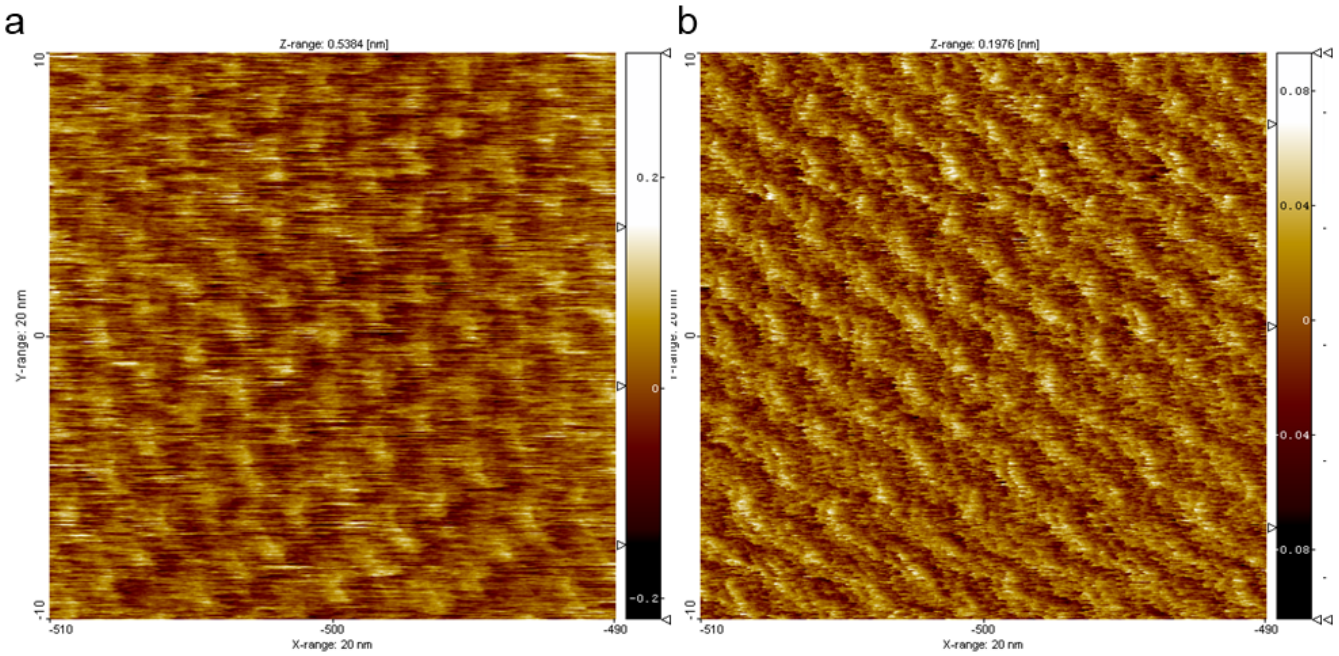

Fig. S 13 Representative AFM images of **CC3**-*R*, (a) showing contact mode topography and (b) simultaneously recorded friction images.

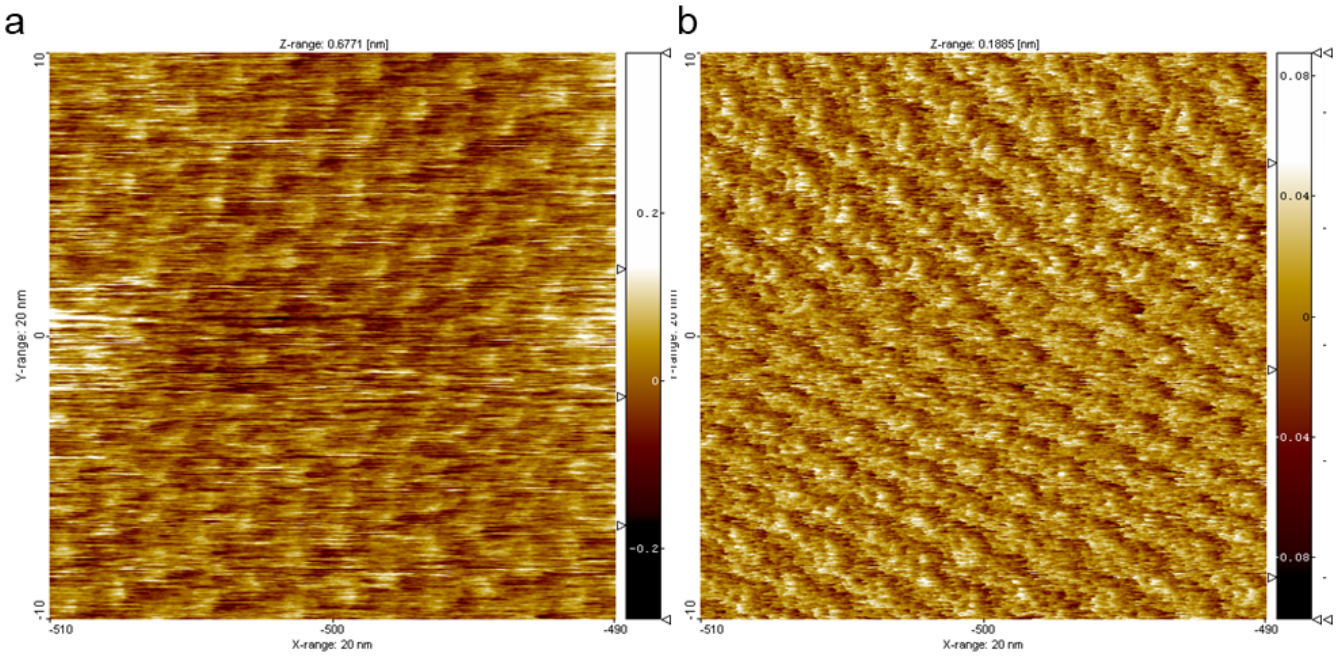

Fig. S 14 Representative AFM images of **CC3**-*R*, (a) showing contact mode topography and (b) simultaneously recorded friction images.

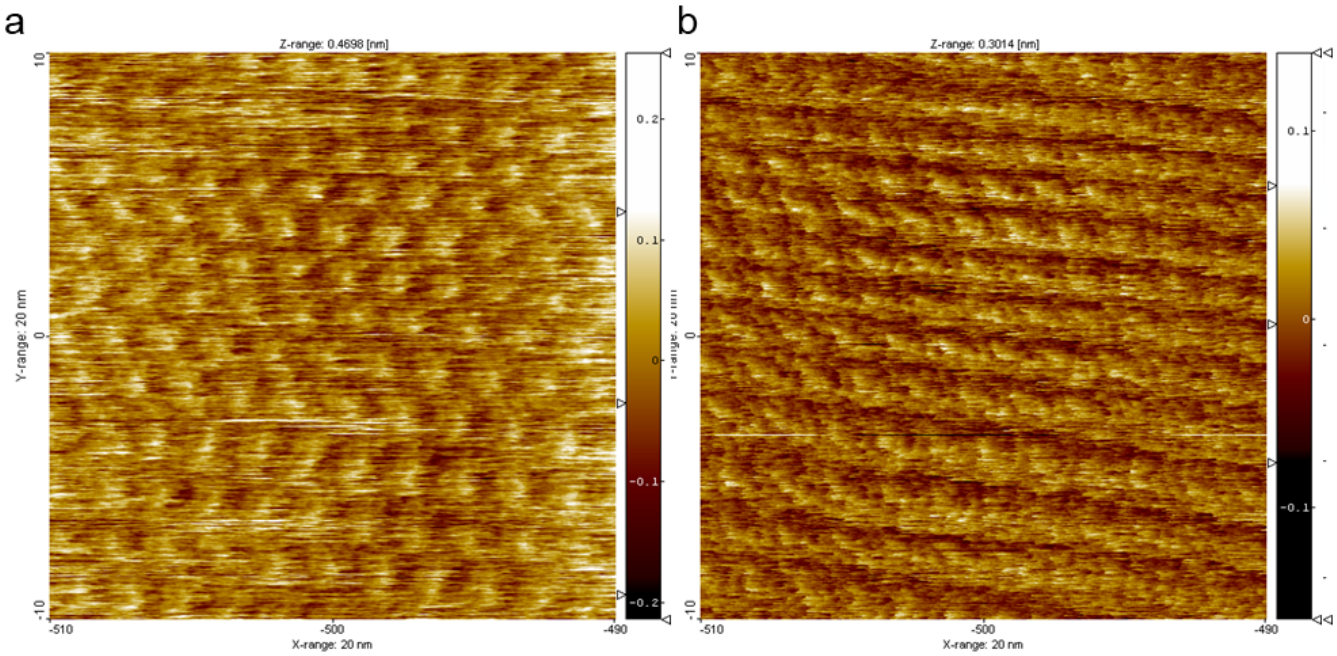

Fig. S 15 Representative AFM images of **CC3**-*R*, (a) showing contact mode topography and (b) simultaneously recorded friction images.

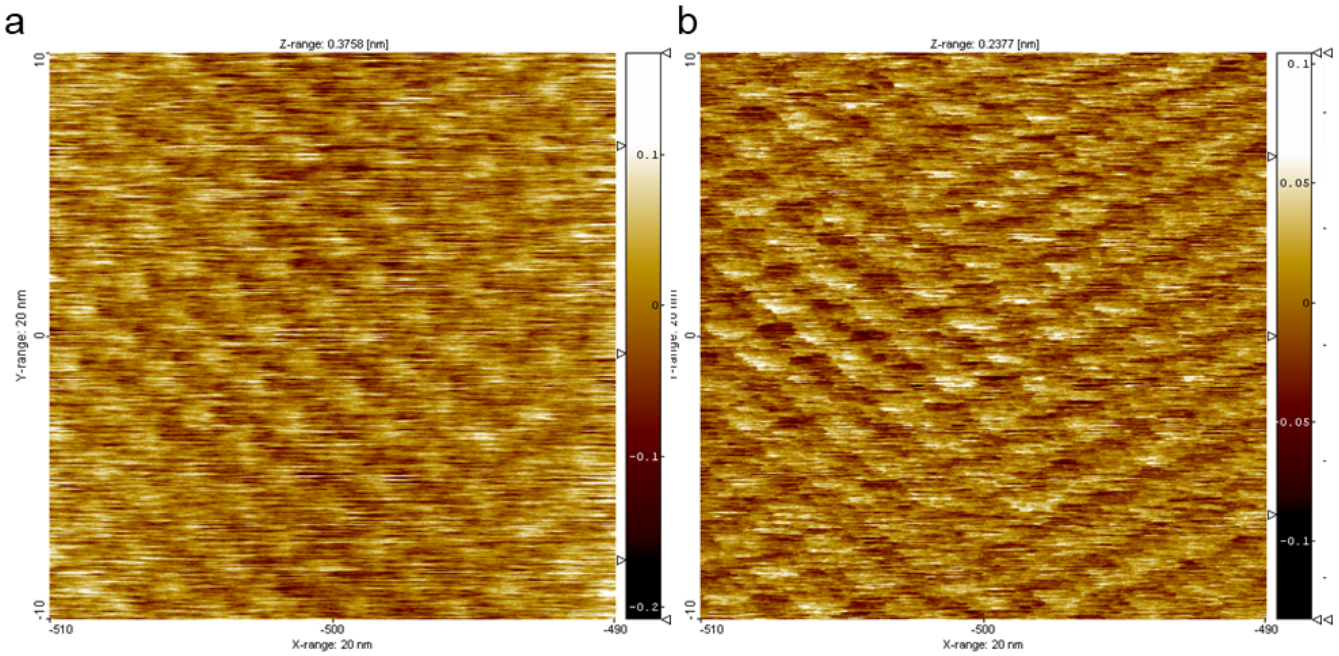

Fig. S 16 Representative AFM images of **CC3**-*R*, (a) showing contact mode topography and (b) simultaneously recorded friction images.

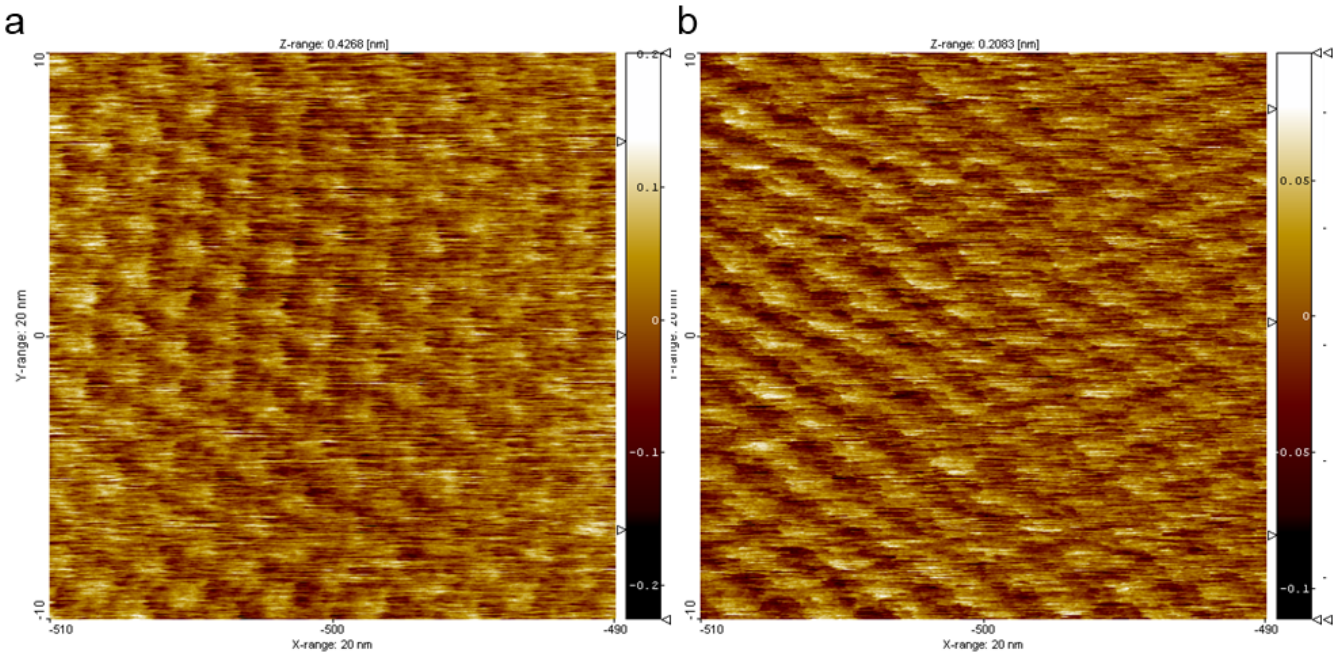

Fig. S 17 Representative AFM images of **CC3**-*R*, (a) showing contact mode topography and (b) simultaneously recorded friction images. Although an increase of applied force beyond 12 N/m gives a better resolution, resulting surface damage is visible in the upper part of the scan area.

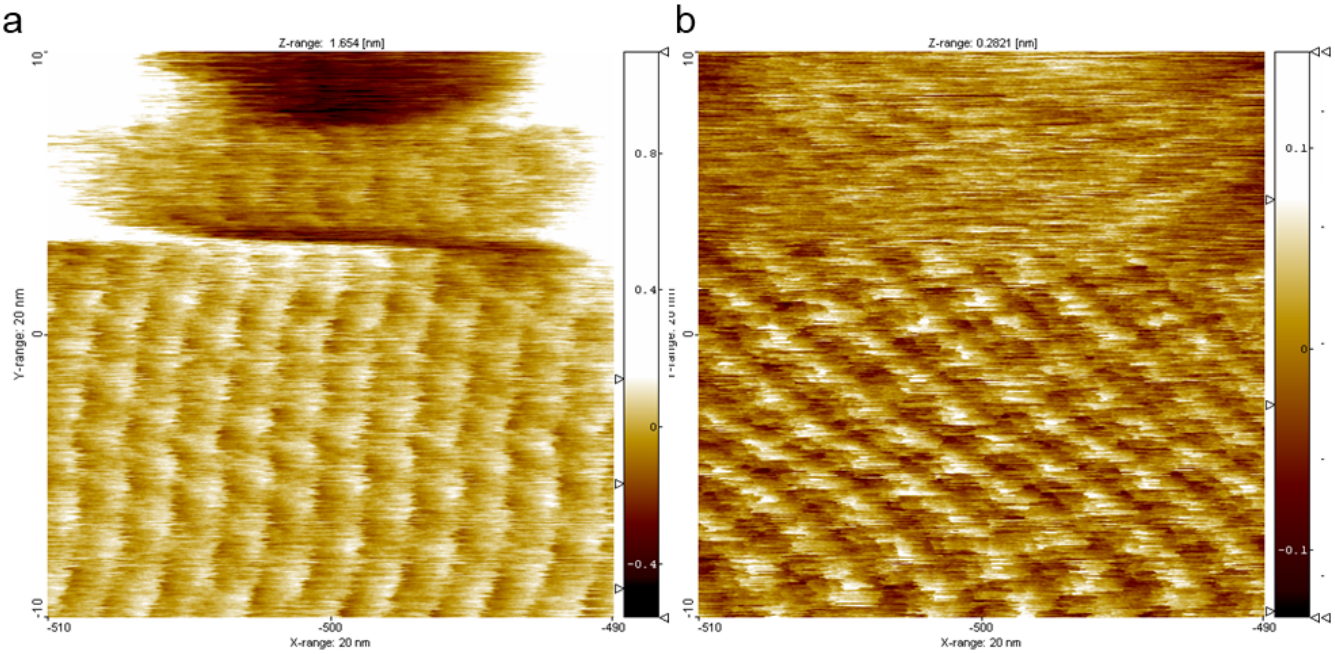

Fig. S 18 (a) Representative contact mode topography AFM image of the (-1 -1 -1) face of **CC3**-*R*. (b) Contour map of Fig. S14a generated with WSxM 3.0 Scanning Probe Microscopy Software after Gaussian smoothing (X and Y decay distance of 5 matrix points).

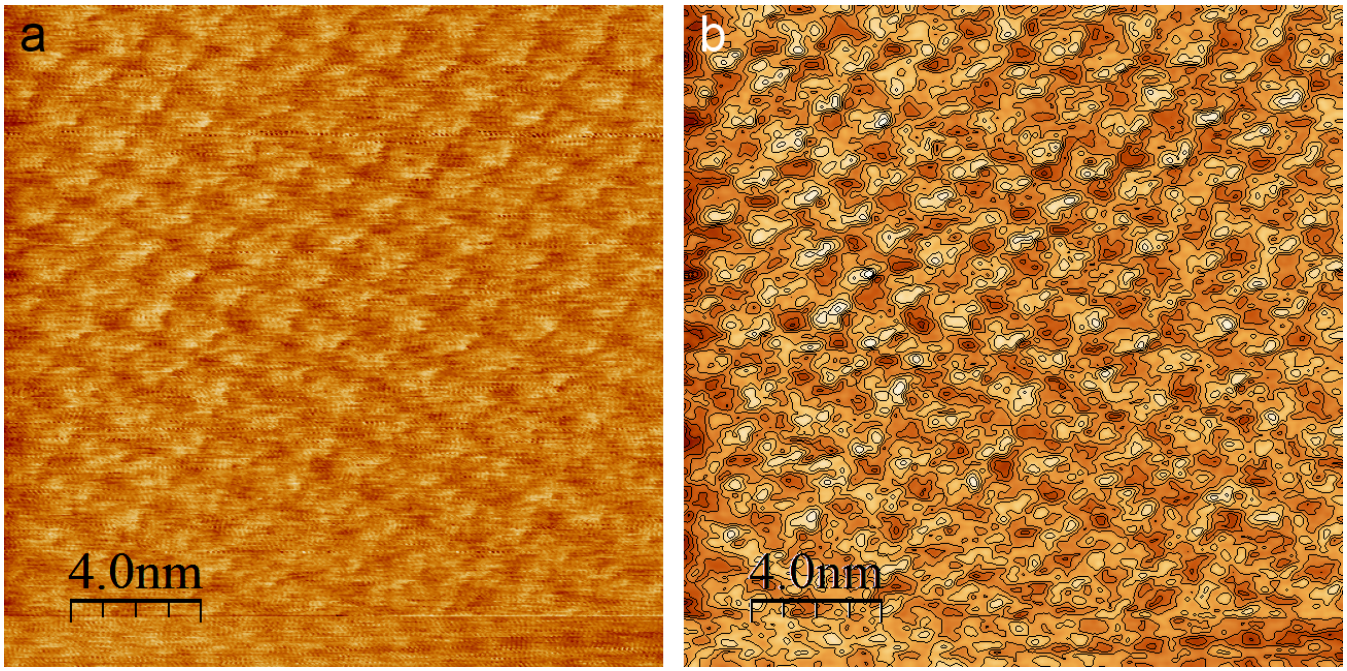

Fig. S 19 (a) Representative contact mode topography AFM image of the (1 1 1) face of **CC3**-*R*. (b) Contour map of Fig. S15a generated with WSxM 3.0 Scanning Probe Microscopy Software after Gaussian smoothing (X and Y decay distance of 5 matrix points).

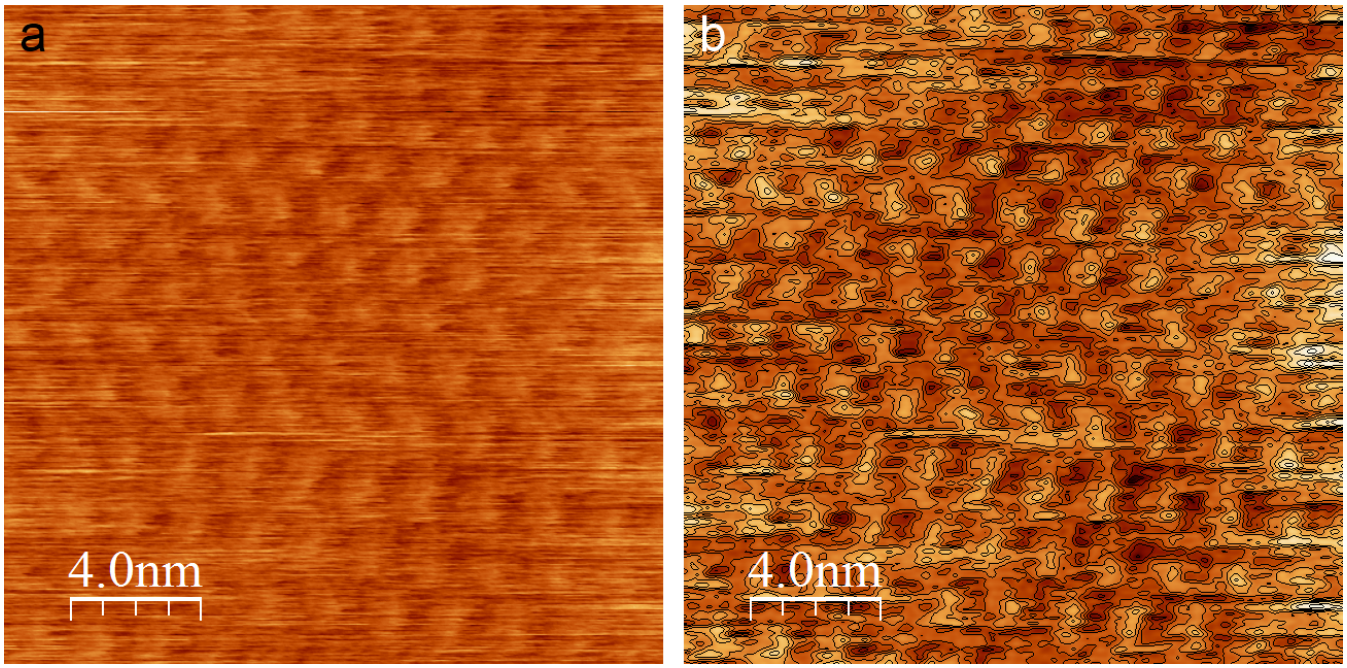

Fig. S 20 Software zoom on a contact mode topography AFM image of the (-1 -1 -1) face of **CC3**-*R*. Contour map generated with WSxM 3.0 Scanning Probe Microscopy Software after Gaussian smoothing (X and Y decay distance of 5 matrix points). The distances between hills correspond to the expected distances between the exposed cyclohexyl vertices across one cage (1.11 nm) and across the inter-cage space (0.75 nm).

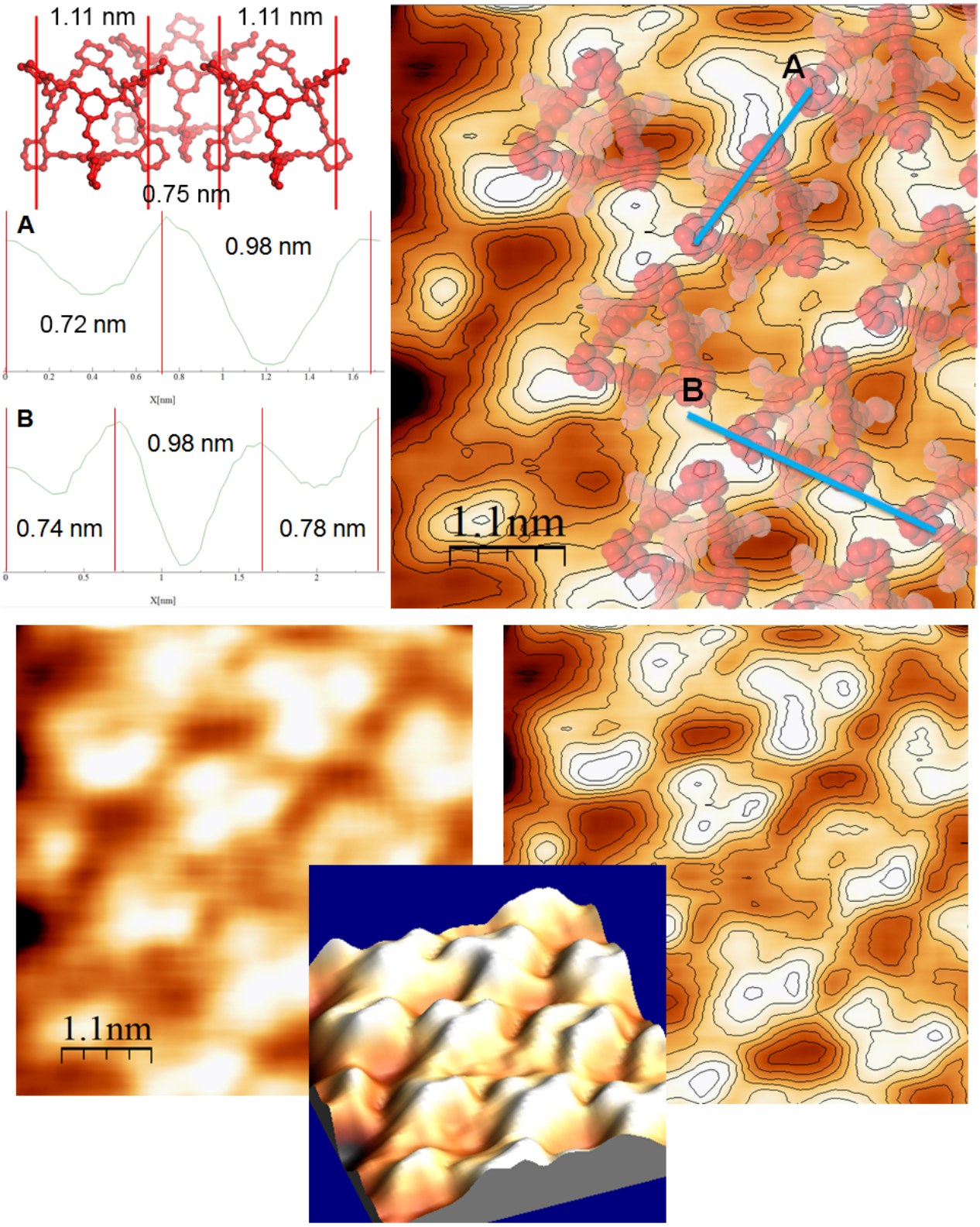

References:

[1] D. Holden, K. E. Jelfs, A. I. Cooper, A. Trewin and D. J. Willock, *The Journal of Physical Chemistry C*, 2012, **116**, 16639-16651.

[2] Hasell, T.; Chong, S. Y.; Jelfs, K. E.; Adams, D. J.; Cooper, A. I. *Journal of the American Chemical Society*, 2012, **134**, 588.